COMBINED GROUND DEFORMATION STUDY OF BROADER AREA OF PATRAS GULF (W. GREECE) USING PSI-WAP, DGPS AND SEISMICITY ANALYSES

Vassilis Sakkas [(1)], Nico Adam [(2)], Panagiotis Papadimitriou [(1)], Nikolaos Voulgaris[(1)], Spyridoula Vassilopoulou[(1)], Brian N. Damiata [(3)], Evangelos Lagios [(1)], Salvatore Stramondo [(4)]

[(1)] Department of Geophysics-Geothermics, University of Athens, Panepistimiopolis-Ilissia, 15784 Athens, Greece. Email: vsakkas@geol.uoa.gr
[(2)] German Aerospace Center (DLR), Remote Sensing Technology Institute, SAR Signal Processing, Oberpfaffenhofen, 82234 Weßling, Germany. Email: Nico.Adam@dlr.de
[(3)] Cotsen Institute of Archaeology, University of California, Los Angeles, CA 90095-1510, USA. Email: damiata@ucla.edu
[(4)] Istituto Nazionale di Geofisica e Vulcanologia National Earthquake Center Remote Sensing Laboratory Via di Vigna Murata 605, 00143 Rome, Italy, Email: salvatore.stramondo@ingv.it

ABSTRACT

Long-term ground deformation monitoring using the Persistent Scatterer Interferometry Wide Area Product (PSI-WAP) technique for the period 1992-2003, combined with Differential GPS measurements and seismicity analysis has provided useful information about the tectonic motions of the tectonically complex area of Patras Gulf (Western Greece), and lead to new insights on the geotectonic regime of this region. Descending ERS radar images were used to compile the PSI-WAP product that has been calibrated using the absolute velocity field of available GPS stations in the area. It has been found that the deformation of the southern part of Patras Gulf near the coastline has been characterized by considerable subsidence (>-5mm/yr), where unconsolidated sediments usually prevail, compared to the northern part of the gulf. Significant subsidence has also been identified in areas along the down-throw side of possible faults, as well as areas where extensive ground water pumping has occurred for irrigation. These results correlate well with local GPS and seismicity data.

1. BRIEF GEOTECTONIC SETTING

The Eastern Mediterranean is one of the most active tectonic areas in the world [1], resulting from the convergence between the Eurasian and the African continental plates. The majority of the seismic activity is located in the Hellenic territory along the Hellenic Arc, the subduction zone of the African plate beneath the Aegean microplate, with the highest activity observed on the western part of the arc that includes the Central Ionian Islands [1]. Due to the compressional forces applied in the Aegean lithosphere, resulting in a southwestward (relative to Eurasia) movement of the plate, the Aegean domain undergoes crustal extension in a marginal basin environment behind the active subduction system of the Hellenic outer arc. This extensional stress field is concentrated in several zones of graben development, both in front and behind the active volcanic inner arc of the Aegean.

In the following, a brief description of the main geotectonic setting is summarized (after [2]). Thrusting of basement and sedimentary rocks is currently active beneath the Hellenic Trench while thin-skinned deformation of sedimentary strata, detached mainly within Triassic salt horizons, occurs outboard of the trench, but does not appear to involve the underlying basement [3]. Extensional faults and linked strike-slip faults of the Central Hellenic Shear Zone cut and disrupt these underlying nappe structures [4], but the converse is not generally observed [5]. These relations also indicate that the extension and strike-slip faulting near the western coast of mainland Greece probably did not begin until Pliocene time [6].

The morphology of the study area reflects the older structures created by thrusting in the Hellenides and also the younger, superposed structures that disrupt them. The broad topographically high areas of western Greece generally correspond to regions of crustal thickening which developed in tandem with thrust faulting and folding. Here, thrust faults and associated folds typically trend NW to NNW, sub parallel to the Hellenic trench. A detailed geological map of the broader area of Patras Gulf is depicted in Fig. 1. It can be seen that alluvial deposits are prevalent in low-lying regions, while limestones of various ages are characterizing the mountainous areas.

2. SEISMICITY ANALYSIS

The broader area of Patras Gulf is a very active tectonic area (Fig. 2) that is characterized by intense seismic activity. A large number of earthquakes of magnitude M_w>5 has occurred in the vicinity of the area over the last 30 years. The most notable large-magnitude seismic events are:

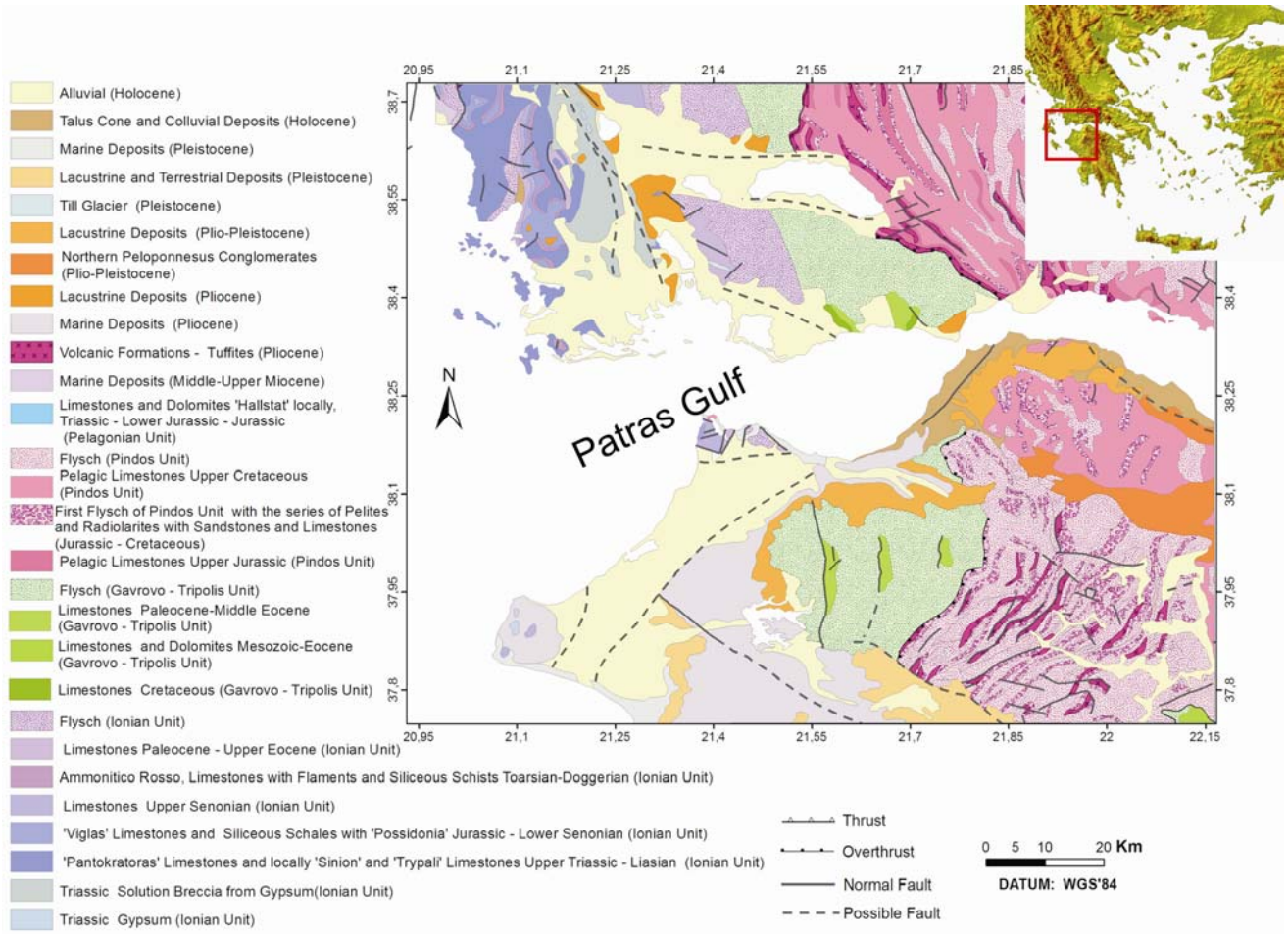

Figure 1. Detailed Geological Map of the broader area of Patras Gulf, showing also the main faulting features (IGME, Geological Map of Greece, 1983)

- 1993: ***Patras*** Earthquake (M_w= 5.4)
- 1995: ***Aegion*** *Earthquake* (M_w=6.4)
- 2002: ***Vartholomio*** *Earthquake* (M_w=5.6)
- 2008: ***Andravida*** *Earthquake* (M_w= 6.4)

The focal mechanisms of these last three major earthquakes have shown a NE-SW trending zone that crosses the area. Several others events have also occurred adjacent and to the west of Patras Gulf, mainly along the Cephalonia Transform Fault and south of Zakynthos Island [7], [8]. A prominent feature of the seismicity map is the absence of activity in the marine area of gulf when compared to the broader region. This absence of seismicity may be indicative of the lack of major faulting systems in the area, or at least active faults. It has to be noted, though, that the submarine area has not been fully mapped.

A major seismic event took place to the east of Patras Gulf in June 1995, the Aegion Earthquake [9]. On June 8, 2008, the Andravida Earthquake, with M_w=6.4 occurred on NW Peloponnese in the vicinity of the Riolos (RLSO) Continuous GPS (CGPS) station (e.g. [10]). Low seismicity was observed in the epicentral area over the past few decades. No historical large events have been reported in this area, where furthermore no evidence of surface faults exists.

Strike-slip faulting has been observed in the surrounding region. The source parameters of the Andravida Earthquake were calculated using body-wave modeling. The focal depth was estimated to be 23 km, while the fault plane solution indicates dextral strike-slip faulting, oriented in a NNE-SSW direction. The slip distribution indicates complex rupture with propagation towards the north. The focal mechanism of the main shock showed a right lateral strike-slip motion. The spatial distribution of the aftershocks covers an area of about 40km in length and oriented in a NNE-SSW direction, in agreement with the constrained focal mechanism of the main shock. The length of the main rupture was approximately 25km, while the aftershock area extends to more than 40km. The seismicity at the two edges of the activated fault can be attributed to stress transfer caused by the main shock, as revealed by Coulomb Stress Analysis [11] in the area.

Note that the causative fault was striking NE–SW and dipping 85°NW. It was of right-lateral slip. Thus, this fault acts as a transition between the extensional area of Patras Gulf–Corinth rift and the compressional area of the Ionian Sea. There is no historical evidence that the 2008 fault segment was ruptured by strong earthquake in at least the last 300 years.

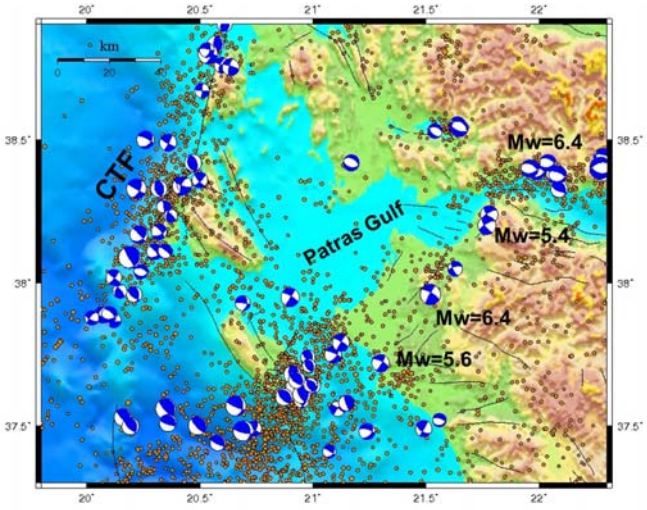

Figure 2. Seismic activity in the broader area of Patras Gulf (M_w>3.6) for the period 1980-2012.

Low seismicity was observed in the epicentral area for the years 1964-2007, setting it as a likely candidate for a forthcoming event [11]. Strike-slip faulting has been observed in the surrounding region, while the type of motion in the study area remained under discussion. More specifically, the two moderate Chalandritsa events (M_w=4.5) occurred NE of the focal area four months before the Andravida Earthquake. In addition, reverse faulting dominates along the Hellenic Arc to the west, while to the NE in the Gulf of Corinth the main active faults are normal with an approximately E-W orientation.

After the occurrence of the Andravida Earthquake, an important number of aftershocks were located using data from the Hellenic Unified Seismological Network (HUSN). The best located events for the period 8-26 June 2008 were 490 [12]. Following, cross-correlation and nearest-neighbor linkage [13] were applied, resulting in several multiple clusters. Finally, relocation was performed [14] with both catalogue and cross-correlation differential travel-time data. The spatial distribution of the relocated aftershocks covers an area of about 40km in length with a NNE-SSW direction, in agreement with the constrained focal mechanism of the mainshock. Fault plane solutions of the largest aftershocks indicate a type of faulting similar to the one of the major event. The length of the main rupture was approximately 25km, while, as previously mentioned, the aftershock area extends to more than 40km. The seismicity at the two edges of the activated fault can be attributed to stress transfer caused by the mainshock, as revealed by Coulomb Stress Analysis [11]. Pick Ground Velocity (PGV) distribution [15] was obtained using the determined slip model. High PGV values between 17 and 20 cm/sec were observed at the northern edge, where many structural damages were reported, but in an area that was not ruptured. The observed damage can be attributed to stress transfer.

3. THE GPS MEASUREMENTS

A GPS network (Fig. 3) was established in the broader area of Patras Gulf in August 1994 to study the crustal deformation, as well as the tectonic settings and motions at both local and regional scales. The Patras Network consists of ten stations equally distributed on both sides of the gulf (5 stations on the northern side and 5 stations on the southern side). The network was fully remeasured on three periods that is in August 1994, in October 1996 and in January 2006. The analysis presented in the following is based on [16]. The Bernese software v.5.0 [17] was used for the post-processing of all the GPS observations. On a regional scale, horizontal and vertical motion of the broader area was estimated with respect to ITRF2000 using data also from the CGPS station RLSO.

A ground deformation having direction of ENE to NE with a rate of 10.6 - 22.2 mm/yr was observed for the northern part of Patras Gulf (Fig. 3a). The southern part exhibited an ESE to SE displacement with rate of 6.3-11.6 mm/yr. Concerning the vertical component, uplift was generally observed. The rate was about 3 mm/yr in the northern part of the gulf, while in the southern part the rate was higher ranging from 5.9-12.1 mm/yr (Fig. 3b). A distinct differential movement between the northern and the southern parts of the gulf is apparent from these images. An opening up of the gulf is evident from the horizontal vector, while the vertical component indicates uplift of the southern part compared to the northern part.

The horizontal deformation vectors revealed an extension of the Patras Gulf: The southern part seems to be extending towards the SSW direction with a rate of 8-13 mm/yr, while in the north, there is a clear differentiation between the westernmost part (station No 35) and the eastern part. The main N-S faulting zone that crosses the area seems to affect these movements. The absence of seismic activity in the marine area of the gulf shows that the extension that takes place in the area is of an aseismic/plastic character on a soft soil environment, without active faulting zones. These results are consistent with geological [18], tectonic [19], seismological [9] and other GPS studies [20] in the area. Previous studies determined that the extension rate increases from 5 mm/yr at the eastern Corinth Gulf to

15 mm/yr on the west, near Aegion (e.g.[20]). A mean extension rate in the Patras Gulf of 8-10 mm/yr was determined based on the tectonic evolution of the area [4], while 20-30 mm/yr of dextral strike-slip occurs along the Cephalonia Transform Fault (e.g [8], [9], [20]).

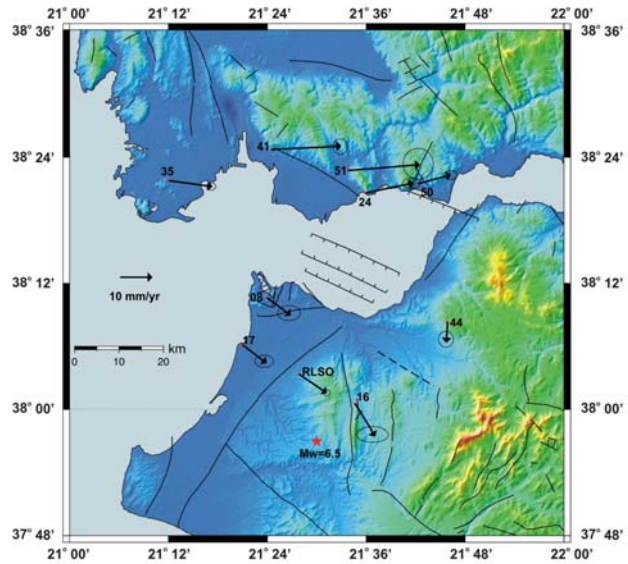

(a)

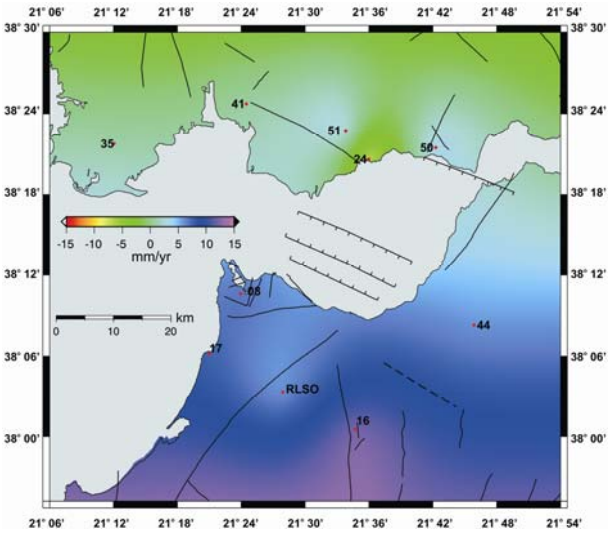

(b)

Figure 3. ***(a)*** *Horizontal and* ***(b)*** *Vertical velocity rates (mm/yr) of the Patras Gulf GPS network observed for the period 1994-2006 (ITRF2000) (after [16]).*

The horizontal strain rate field was calculated based on the horizontal velocities of the area [21], and is depicted in Fig. 4. *Blue* arrows describe extension, while *Red* arrows compression. The most important feature is the extension in the western part of Patras Gulf that decreases in the eastern part close to the Rio-Antirrio Bridge. The eastward decreasing extension of gulf is consistent with previous research, and is attributed to the counter-clockwise rotation of the Peloponnese relative to the mainland of Greece, around a pole located in the Saronic Gulf to the south of Athens [22].

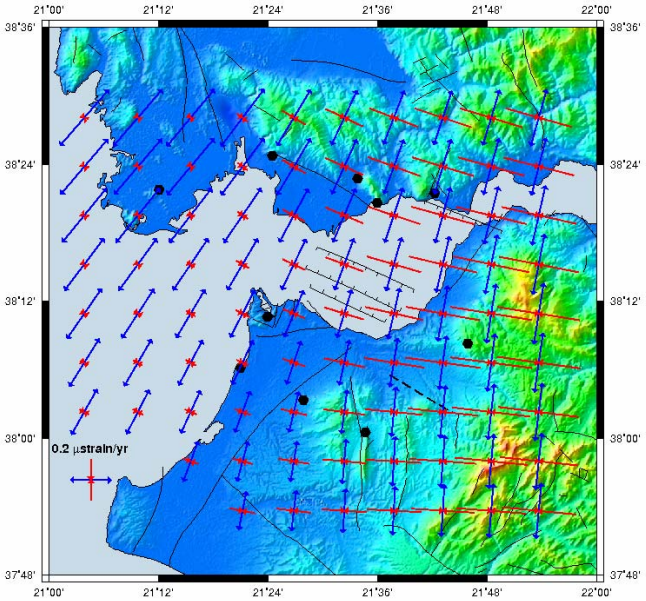

Figure 4. Strain Field Distribution in the broader area of Patras Gulf deduced by GPS observations for the period 1994-2006.

4. THE PSI-WAP METHODOLOGY

The Persistent Scatterer Interferometric (PSI) technique [23], [24] is a powerful method to measure surface deformation at a millimeter accuracy based on radar remote sensing. PSI is an established technique for measuring subtle deformation in urban areas over regions of about 10km by 10km and at a density of about 100 scatterers/km^2. This technique was adapted by DLR for the processing of "wide areas" and the new product is called Wide Area Product (WAP) [25]. The WAP uses full frame ERS acquisitions with dimensions of about 100km by 100km and up to 1,000,000 points as a building block. The final product is a mosaic of full frames and can cover a country or even continents. The measurement points (PSs) in a WAP are distributed irregularly and inhomogeneously due to the rare and by chance occurrence of man-made features in rural areas. Furthermore, the phase stability of the detected PSs is typically worse in rural areas as compared to urban areas. This new data characteristic requires an updated algorithm of the PSI processor in order to avoid spatial error propagation, and meet the end-user requirements and expectation on the monitoring precision.

The results of the InSAR processing are co-registered interferograms with a wrapped phase for each pixel (i.e. it is modulo 2π). For the determination of the parameters of interest at stable scatterers (topography update and deformation), the Spatial and Temporal

Unwrapping Network (STUN) algorithm [26] was developed at DLR-IMF. The first step in this procedure is the detection of Persistent Scatterer Candidates (PSCs). Afterwards, a reference network between stable scatterers over a sparse grid is established for the entire scene. Finally, all detected points are estimated relative to the reference network.

The possibility to interface and merge the PS results with additional measurements is a key point in the developing of an operational processor. The idea is to exploit results provided by other sensors/instruments in order to overcome the limitations of the PSI. These limitations can be intrinsic in the methodology (e.g., impossibility to have an absolute measure of the deformation), or specifically of the single processing (e.g., presence of not connectable PS clusters at the end of the processing). In the framework of the development of the WAP, a general concept for the absolute calibration of the PSI measures using GPS stations was introduced.

Assuming that for the area of interest there are displacement vectors from GPS stations for the same time span of the SAR acquisitions, and since the very "low-pass" deformations phenomena are not measurable by the PSI technique, GPS measurements may be used to keep track of such effects. A map may be generated as the reference on which the PSI results will be calibrated. If the overlap between the GPS stations and the PS results is not sufficient (i.e., at least 1 station per PS cluster +2 in order to detect eventual trends), it will be necessary to interpolate the measurements. As far as the GPS is supposed to provide only the very large scale deformations, the interpolation of the results should not be particularly critical and can be carried out using typical methods (e.g. Kriging).

The deformation measured from the GPS station is normally provided in terms of the three components North, East and Vertical. In order to make them comparable to the interferometric geometry, it is necessary to project these components in the radar's Line of Site (LOS) direction. This operation depends on the position of the GPS measurements in the scene (Latitude, Longitude and Altitude) and from the SAR sensor position at the same time instant; therefore, it has to be performed for every station/measure independently. The computation has to be computed in X,Y,Z coordinates as far as the state vectors of the satellites that contain the positions of the platform during the acquisition are provided in this reference system.

ERS1 and ERS2 satellite data were used for the compilation of the PSI-WAP product carried out by DLR. Sixty six descending satellite geometry ERS radar images were used covering an area of about 106km by 119km and with a density of about 6.9 PS/km^2 (Fig. 5) for the period November 1992 to November 2003. About 98,000 PSs were identified. Initially, the delivered non-calibrated PSI products were composed of independently estimated clusters. Each cluster is referred to its own reference point. The selected points guaranteed the best quality for the processing of the radar imagery, presenting thus a low-noise time series and consequently a noise reduction of the data set. However, the absolute deformation of the study areas was deduced by incorporating the ground deformation velocities based on GPS analysis, which were considered in the present study.

5. THE PSI-WAP DESCRIPTION

Considering the GPS calibrated PSI results for the study area, the reader has to have in mind that the ground deformation velocities resulted in the WAPs are motions along the satellite LOS. Due to the radar incident angle (about 23^o), the vertical component of the deformation vector is more than 90%. For this reason, hereafter, the terms 'subsidence' and 'uplift' have been adopted to describe the motions of the PSI points. Fig. 5 represents the LOS velocity field in the broader area of Patras Gulf. It can be seen that most of the PS points are associated with urban areas (e.g., cities of Patras, Messologion etc.) and limestone outcrops (refer to Fig. 1). Most of the PS points are identified in mountainous regions.

It is noted that the regional motion of the area, according to the GPS results, is to the SW with respect to Europe with a rate of about 25 mm/yr [20], without taking into account the vertical component; this is because no estimate of that component is provided by the published data. Therefore the calibrated PSI-WAP has a negative inherent component that describes a motion ***away*** from the satellite. The former inevitably causes an increase in the LOS distance at each identified PS point, thus yielding a fictitious overall apparent "*subsidence"* of the area as presented in the image.

Considering the southern part of Patras Gulf (Fig. 5), the majority of the PS points located near to the coast indicate subsidence varying from -2 to -5 mm/yr and locally exceeding -7 mm/yr. These PS points, as may be seen from the geology (Fig. 1), have been identified on alluvial deposits, as well as in marine deposits. The western part shows a significant subsidence (more than -3 mm/yr), and is associated (i) with marine deposits and alluvial deposits, and (ii) extensive ground water pumping for irrigation. Considering the NE part that mostly coincides with the City of Patras, a differential motion is noticed across and along the identified SW-NE running fault. Its northern part strongly subsides, while its southern part appears to subside but at a lower rate. The remaining PS points in this area towards the

south are located on limestones and flysch showing rather smaller rates of subsidence (about -3 mm/yr) or even stability (> -1 mm/yr).

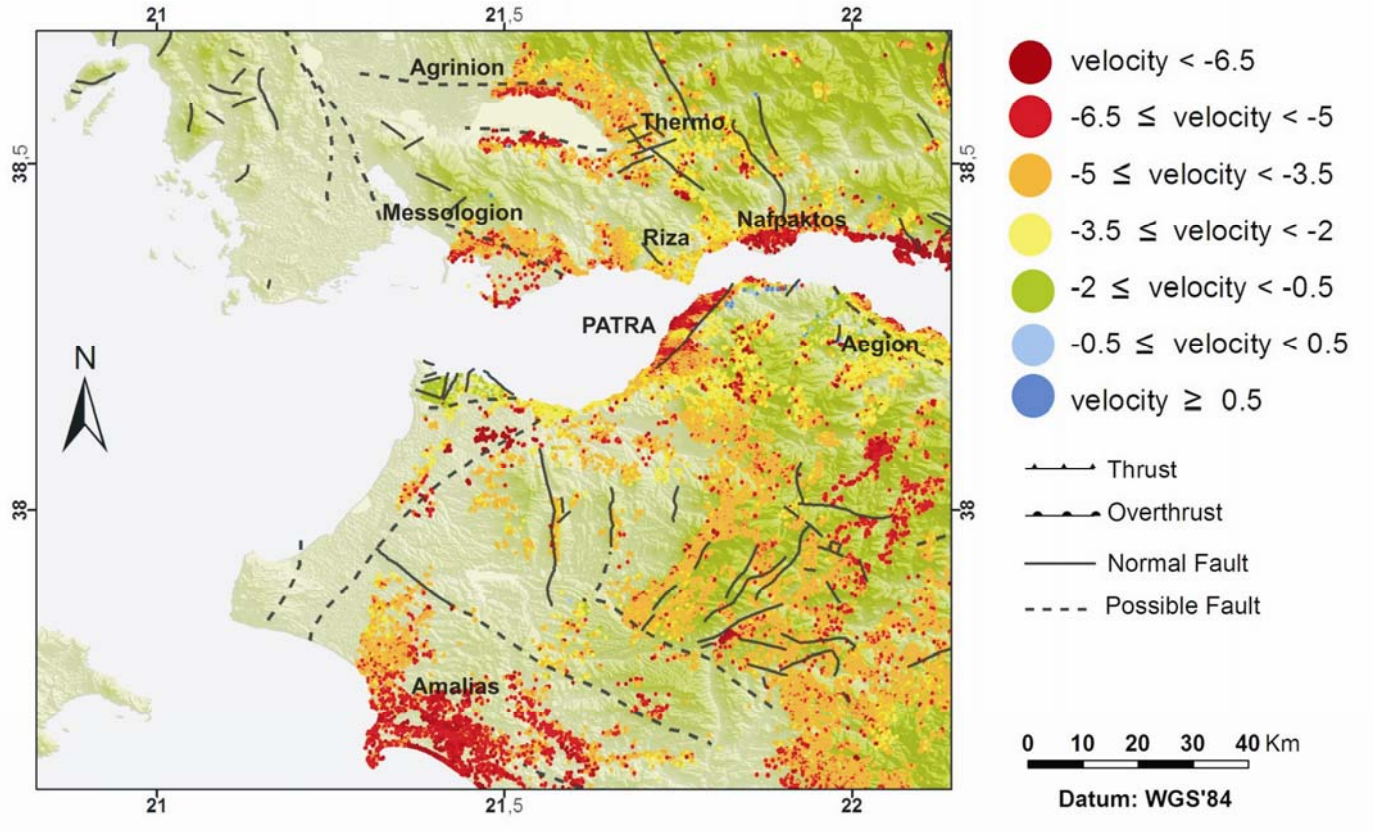

Figure 5. PSI-WAP image of the broader area of Patras Gulf (Western Greece) (velocity in mm/yr).

The PS points at the SE part are located on a succession of Cretaceous Limestones and Pindos Flysch that show alternating moderate values of subsidence associated with local faults. Particularly in the extreme SE part, all PS points are identified on the Pindos Flysch unit and not on the adjacent Tripolis Flysch unit (Fig. 1). Mainly subsidence is observed associated with a region where a series of NE-SW trending faults prevail with parallel intrusions of volcanic tuffs. These flysch formations may be pertinent to landslides that may explain the observed subsidence. Amalias Town shows a consistent pattern of subsidence, where the geology consists mainly of Palaeocene Limestones and adjacent alluvial formations. Extensive irrigation is a significant factor contributing to the observed subsidence.

Fewer PSI points are noted at the northern part of Patras Gulf, and are mostly associated with urban areas, such as the cities of Agrinion, Messologion, Nafpaktos, and the villages of Riza and Thermo, and limestone outcrops (Fig. 1). It can be seen in the Nafpaktos area that the observed subsidence (more than 5 mm/yr) starts taking place when moving from the Pindos Jurassic Limestone unit on the North to alluvial deposits in the plane fields on the South. This area is associated with the Aegion Earthquake (M=6.4) in 1995 (Fig. 2), and its influence cannot be excluded. The Riza area is associated with the Palaeocene Tripolis Limestone unit which shows a more stable image compared to the surroundings, since the PS points vary from -2 to -3 mm/yr. A similar deformation is observed also at Thermo Town, where the geology consists mainly of Pindos Limestones, including a small area of recent sediments (alluvium).

At Agrinion and Messologion, similar geodynamic characteristics are observed. Both cities are situated on alluvial deposits that are adjacent to limestone/flysch formations, and on the down-throw side of possible faults (Fig. 1). PS points located on limestone/flysch formations seem to show small subsidence, while those situated on alluvial deposits seem to strongly subside. The results of our GPS stations in Riza and Messologion (Fig. 3) for an overlapping period (1994-2006) are not consistent with the observed PSI in these areas, showing a slight uplift (about 3mm/yr) and a small subsidence (about -2mm/yr), respectively.

Given that the seismicity is at a low level (Fig. 2) in the northern part of Patras Gulf (with the exception of the area to the east of Rion-Antirrion – the boundary between the Patras and Corinth Gulfs – Nafpaktos area) for the period (of the PSI-WAP) 1992-2003, the ground

deformation should rather be attributed to local geological and tectonic features, including locally some human activity (water pumping for irrigation). However, at the southern part of Patras Gulf, the strong seismicity that is taking place (Fig. 2) should rather be to some extent contributing to the observed ground deformation affecting mainly the coastal areas, where unconsolidated sediments usually prevail. This argument is supported by the damages caused in the aforementioned areas by the occurrence of the Andravida Earthquake that took place in 2008, well after the spanning period of the WAP.

6. DISCUSSION – CONCLUSIONS

Extensive multi-disciplinary work has been conducted in the Corinth Gulf over the past twenty years, because it is a very seismotectonically active area. However, the adjacent Patras Gulf on the West has not been studied in such detail. Therefore, the present work is a contribution to the study of this active area and attempts to infer probable tectonic issues resulting from the ground deformation as deduced by the WAP.

The GPS observations on both sides in the Patras Gulf were able to identify regional motions for the period 1994-2006 relating to the *opening* of the Gulf with a rate of about 8-10 mm/yr, and the differential *vertical* motion between the northern and the southern parts. The southern part has uplifted faster than the northern part at a rate of about 8-10 mm/yr. However, such regional motions cannot be confirmed by the PSI WAP, since the identified PS points show ground deformation only along the LOS direction. Besides the calibrated PS points have not taken into consideration the vertical component which was assigned as zero, while our local CGPS station RLSO showed a constant uplift of about 5 mm/yr [16]. Nevertheless, both GPS and PSI methodologies may be integrated contributing to the better understanding of the tectonics. Even though most of the identified PS points deduced by the WAP have been located in urban environments, significant results may be concluded relating to geo-tectonic issues on a larger scale.

The broader area of Patras Gulf shows significant subsidence, probably due to the large GPS velocity values in the area of Patras Gulf (about 25 mm/yr) that were used to calibrate the PSI data. Smaller subsidence has taken place in limestone formations, while stronger subsidence has occurred in alluvial and coastal deposits. The coastal areas of Patras (extending from East to West) have shown a significant subsidence (up to 5 mm/yr) associated with alluvial and coastal deposits, human activity (water pumping for irrigation purpose), and along the downthrown side of the Patras Fault. The western part of this area (Kato Achaia) had suffered extensive damages during the Andravida Earthquake (2008). Therefore, areas of similar geo-tectonic setting and ground deformation pattern may be subjected to the same consequences in case of a future strong earthquake. The high seismicity in the broader area of Patras Gulf may have affected the observed ground deformation (Nafpaktos area), while the former is not evident in the northern part of the gulf where low seismicity has been recorded for the period 1992-2003.

It is believed that the deformation image as deduced by the PSI-WAP combined with seismological, geo-tectonic and GPS data may help to identify areas prone to serious damages in case of future seismic activity.

7. ACKNOWLEDGMENTS

The authors would like to acknowledge the processing effort of the German Aerospace Center (DLR) InSAR team namely Fernando Rodriguez Gonzalez, Alessandro Parizzi and Ramon Brcic. This work was carried out in the framework of the TERRAFIRMA Stage-3 ESA's Program.

8. REFERENCES

1. McKenzie, D. (1978). Active tectonics of the Alpine-Himalayan belt: the Aegean Sea and surrounding regions, *Geophys. J. R. astr. Soc.* 55, 217-254.

2. Vassilakis, E., Royden, L. & Papanikolaou, D., (2011). Kinematic links between subduction along the Hellenic trench and extension in the Gulf of Corinth, Greece: A multidisciplinary analysis. *Earth Planet. Sci. Lett.* 303, 108-120.

3. Underhill, J.R. (1989). Late Cenozoic deformation of the Hellenide foreland, western Greece. *Bull. Soc. Geol. Am.* 101, 613-634.

4. Flotté, N., Sorel, D., Müller, C. & Tensi, J. (2005). Along strike changes in the structural evolution over a brittle detachment fault: Example of the Pleistocene Corinth-Patras rift (Greece), *Tectonophysics* 403 (1-4), 77-94.

5. Papanikolaou, I. & Lekkas, E. (2008). Lithostratigraphic differentiation of the Gavrovo and the Ionian flysch in the Southern Akarnania and the role of the Agrilia and Evinos transverse fault zones. *Hell. J. Geosci.* 43, 41-55.

6. Papanikolaou, D., Fountoulis, I. & Metaxas, C. (2007). Active faults, deformation rates and Quaternary paleogeography at Kyparissiakos Gulf (SW Greece) deduced from onshore and offshore data. *Quaternary International* 171-172 (SPEC. ISS.),. 14-30.

7. Lagios, E., Sakkas, V., Papadimitriou, P., Damiata, B.N., Parcharidis, I., Chousianitis K. & Vassilopoulou, S. (2007). Crustal deformation in the Central Ionian Islands (Greece): Results from

DGPS and DInSAR analyses (1995-2006). *Tectonophysics* 444, 119-145.

8. Lagios, E., Papadimitriou, P., Novali, F., Sakkas, V., Fumagalli, A., Vlachou, K. & Del Conte, S. (2012). Combined Seismicity Pattern Analysis, DGPS and PSInSAR Studies in the Broader Area of Cephalonia (Greece). *Tectonophysics* 524-525, 43-58.

9. Bernard, P., Briole, P., Meyer, B., Lyon-Caen, H., Gomez, J.M., Tiberi, C., Berge, C., Cattin, R., Hatzfeld, D., Lachet, C., Lebrun, B., Deschamps, A., Courboulex, F., Larroque, C., Rigo, A., Masonnet, D., Papadimitriou, P., Kassaras, I., Diagourtas, D., Makropoulos, K., Veis, G., Papazissi, K., Mitsakaki, C., Karakostas,V., Papadimitriou, E., Papanastassiou, D., Chouliaras, M. & Savrakakis, G. (1997). The Ms 6.2, June 15, 1995 Aigion earthquake (Greece): evidence for low angle normal faulting in the Corinth Rift. *J. Seismol.* 1, 131-150.

10. Ganas, A., Serpelloni, E., Drakatos, G., Kolligri, M., Adamis, I., Tsimi, Ch. & Batsi, E., (2009). The Mw 6.4 SW Achaia (Western Greece) Earthquake of 8 June 2008: Seismological, Field, GPS Observations, and Stress Modelling. *J. Earthq. Eng.* 13 (8),1101-1124.

11. Papadimitriou, P. (2008). Identification of seismic precursors before large earthquakes: Decelerating and accelerating seismic patterns. *J. Geophys. Res*. 113, B04306, doi:10.1029/2007JB005112.

12. Papadimitriou, P., Agalos, A., Moshou, A., Kapetanidis, V., Karakonstantis, A., Kaviris, G., Kassaras, I., Voulgaris, N. & Makropoulos, K., (2010). An important number of recent significant earthquakes in Greece, 3*2nd General Assembly of the ESC 2010*.

13. Kapetanidis, V., Papadimitriou, P. & Makropoulos K. (2010). A cross-correlation technique for relocation of seismicity in the western Corinth rift. *Bull. Geol. Soc. Greece, Patras* XLIII (4), 2015-2025.

14. Karakonstantis, A. & Papadimitriou, P. (2010). Earthquake relocation in Greece using a unified and homogenized seismological catalogue, *Bull. Geol. Soc. Greece, Patras* XLIII (4), 2043-2052.

15. Bouchon M. (1981). Simple method to calculate Greens functions for elastic layered media. *BSSA* 71 (4), 959-971.

16. Vlachou, K., Sakkas, V., Papadimitriou, P. & Lagios, E., (2011). Crustal Deformation Studies in the seismically active area of Patras Gulf (Greece). 2011 IEEE Int. Geosci. *Remote Sens. Symp. (IGARSS)*, 10.1109/IGARSS.2011.6050082.

17. Dach, R., Hugentobler, U., Fridez, P. & Meindl, M. (2007). *Bernese GPS Software Version 5.0,* Astronomical Institute, University of Bern.

18. Sébrier, M. (1977). Tectonique récente d'une transversale a l'arc égéen. Le golfe de Corinthe et ses régions périphériques. Thèse de 3eme cycle," Univ. Paris XI – Orsay, France, pp. 137.

19. Jackson, J.A., Gagnepain, J., Houseman G., King G., Papadimitriou P., Soufleris, C. & Virieux, J. (1982). Seismicity, normal faulting, and the geomorphological development of the Gulf of Corinth (Greece): the Corinth earthquakes of February and March 1981, *Earth Planet. Sci. Lett.* 57 (2), 377-397.

20. Hollenstein, Ch., Müller, M.D., Geiger, A. & Kahle, H.-G. (2008). Crustal motion and deformation in Greece from a decade of GPS measurements, 1993–2003, *Tectonophysics* 449, 17-40.

21. Pesci A. & Teza G., (2007). Strain rate analysis over the central Apennines from GPS velocities: the development of a new free software. *Bollettino di Geodesia e Scienze Affini* 56, 69-88.

22. Le Pichon, X., Chamot-Rooke, N., Lallemant, S., Noomen, R. & Veis, G., (1995). Geodetic determination of the kinematics of Central Greece with respect to Europe: implications for Eastern Mediterranean tectonics, *J. Geophys. Res.* 100 (12), 675-690.

23. Ferretti, A.; Prati, C. & F. Rocca, (1999). Permanent Scatterers in SAR Interferometry, *Proc. of IGARSS 1999*, Hamburg, Germany, pp. 1528-1530.

24. Ferretti, A.; Prati, C., Rocca, F., (2000). Permanent Scatterers in SAR Interferometry, *IEEE Trans. Geosci. Remote Sensing* 38, 2202-2212.

25. Liebhart, W., Bricic, R., Parizzi, A., Gonzalez, F.R. & Adam, N. (2012). *PSI-WAP Methodology and Final Characteristics*. DLR WAP Report, 58 pp..

26. Kampes, B. M. (2006). *Radar Interferometry -- The Persistent Scatterer Technique*, Springer, 211pp.